Accepted Manuscript

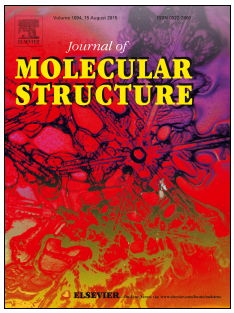

Synthesis, characterisation, estimation of ground-and excited-state dipole moments using solvatochromic shift and theoretical studies of new iminocoumarin derivatives

Amal Rabahi, Malika Makhloufi-Chebli, Sihem Zaater, Meziane Brahimi, Artur M.S. Silva, Baya Boutemeur

PII: S0022-2860(18)31538-2

DOI: https://doi.org/10.1016/j.molstruc.2018.12.105

Reference: MOLSTR 26042

To appear in: *Journal of Molecular Structure*

Received Date: 10 June 2018

Revised Date: 25 December 2018

Accepted Date: 26 December 2018

Please cite this article as: A. Rabahi, M. Makhloufi-Chebli, S. Zaater, M. Brahimi, A.M.S. Silva, B. Boutemeur, Synthesis, characterisation, estimation of ground-and excited-state dipole moments using solvatochromic shift and theoretical studies of new iminocoumarin derivatives, *Journal of Molecular Structure* (2019), doi: https://doi.org/10.1016/j.molstruc.2018.12.105.

Graphical Abstract

To create your abstract, type over the instructions in the template box below.
Fonts or abstract dimensions should not be changed or altered.

Synthesis, Characterisation, Estimation of ground-and excited-state dipole moments using solvatochromic shift and theoretical studies of new iminocoumarin derivatives

Leave this area blank for abstract info.

Amal Rabahi,[a,*] Malika Makhloufi-Chebli,[a,b] Sihem Zaater,[c,d] Meziane Brahimi,[c] Artur M. S. Silva[e,*] and Baya Boutemeur[a]

[a]Laboratoire de Chimie Organique Appliquée (Groupe Hétérocycles), Faculté de Chimie, Université des Sciences et de la Technologie BP32, El-Alia 16111 Bab-Ezzouar, Alger, Algeria; [b]Université Mouloud Mammeri, Faculté des Sciences, Département de Chimie, Tizi Ouzou, 15000 Algeria; [c]Laboratoire de Physico-Chimie Théorique et de Chimie Informatique, Faculté de Chimie Université des Sciences et de la Technologie BP32, El-Alia 16111 Bab-Ezzouar, Alger, Algeria; [d]Ecole Supérieure en Sciences Appliquées (ESSA) Alger, BP 474 Place des Martyrs, Alger, Algeria; [e]QOPNA and LAQV, Department of Chemistry, University of Aveiro, 3810-193 Aveiro, Portugal.

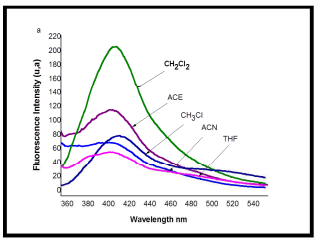

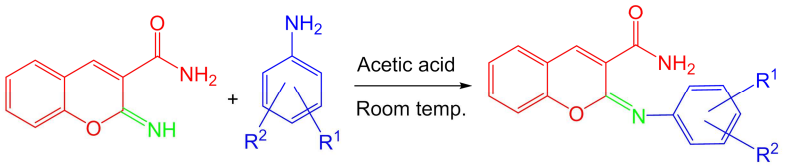

ACCEPTED MANUSCRIPT

Journal of Molecular Structure
journal homepage: www.elsevier.com

Synthesis, Characterisation, Estimation of ground-and excited-state dipole moments using solvatochromic shift and theoretical studies of new iminocoumarin derivatives

Amal Rabahi,[a,*] Malika Makhloufi-Chebli,[a,b] Sihem Zaater,[c,d] Meziane Brahimi,[c] Artur M. S. Silva,[e,*] Baya Boutemeur[a]

[a]*Laboratoire de Chimie Organique Appliquée (Groupe Hétérocycles), Faculté de Chimie, Université des Sciences et de la Technologie BP32, El-Alia 16111 Bab-Ezzouar, Alger, Algeria.*
[b]*Université Mouloud Mammeri, Faculté des Sciences, Département de Chimie, Tizi Ouzou, 15000 Algeria*
[c]*Laboratoire de Physico-Chimie Théorique et de Chimie Informatique, Faculté de Chimie, Université des Sciences et de la Technologie BP32, El-Alia 16111 Bab-Ezzouar, Alger, Algeria*
[d]*Ecole Supérieure en Sciences Appliquées (ESSA), BP 474 Place des Martyrs, Alger, Algeria*
[e]*QOPNA and LAQV, Department of Chemistry &, University of Aveiro, 3810-193 Aveiro, Portugal*

* *Corresponding authors: Amal RABAHI (amal_rabahi@yahoo.fr) and Artur M. S. Silva (artur.silva@ua.pt).*

ARTICLE INFO

Article history:
Received
Received in revised form
Accepted
Available online

Keywords:
Iminocoumarins
Dipole moments
Solvatochromic shift
Intramolecular charge transfer
Theoretical calculations

ABSTRACT

The study on the fluorescence and UV-Vis absorption of some iminocoumarins at ambient temperature in several solvents showed a bathochromic shift with the increase of the solvent polarity. The use of the solvathochromic method allowed us to determine the dipole moment in both ground and excited states. The studied molecules exhibit much higher dipole moments in the excited state than in the ground state, which can be due to the redistribution of π-electron densities in the excited state making molecules more polar with higher dipole moments. Furthermore, HOMO–LUMO gap were also estimated theoretically using B3LYP/6–311+G(d,p) level of theory; the low energy gap indicated the eventual charge transfer interaction occurring in the molecules, and responsible for their light emitting properties.

1. Introduction

Coumarin derivatives attracted the attention of chemists over the past years [1], they constitutes a class of compounds with many biological activities [2-9]. The coumarin derivatives present a great number of biological properties, such as, anti-inflammatory [10], analgesic [11], anti-spasmodic [12], antitumor [13], antimicrobial [14], antibacterial [15], anti-VIH [16] and antioxidant [17] activities. The application of their fluorescence properties are widely known [18-20], being used as fluorescent probes and fluorescent markers in biochemistry [21-22]. Thus, to prepare functionalized coumarins at position 2, we have reacted 2-imino-2*H*-chromene-3-carboxyamide (**1**) with a series of aromatic amines **3**-**10** (Scheme 1).

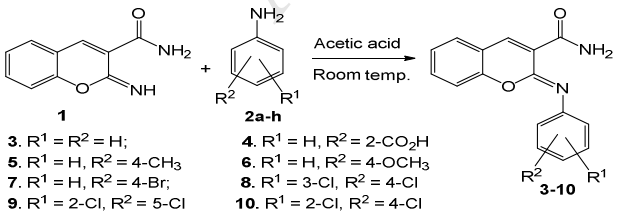

Scheme 1. Synthesis of iminocoumarins **3**-**10**.

We will also describe the ground and excited-state dipole moments of the prepared (2*Z*)-2-arylimino-2*H*-chromene-3-carboxamide derivatives **3-10** calculated from the relation of Lippert, Bakhshiev and Kawski-Chamma-Viallet [23]. The excitation of a compound by absorption of photons causes a redistribution of charges that lead to conformational changes in the excited state. This may result in an augmentation or diminution of the dipolar moment of the excited state relative to that of the ground-state [24]. Prospecting of dipole moments in the ground and excited state of electronically excited molecules provides important information about the electron and geometric structure of the compound in a short-lived state. The knowledge of the excited state dipole moment of electronically excited molecules is very effective to design new compounds with nonlinear optical properties, to elucidate the nature of the excited state and to get the path of their photochemical transformation.

In the absence of crystal structures to determine the most stable conformation of the titled compounds, full-optimized geometry of different rotamers will be carried out. The ground state structures were optimized using density functional theory (DFT) model and employing the hybrid Becke3-Lee-Yang-Parr (B3LYP) functional and at the excited state, structures were optimized by using the time-dependent density functional theory (TD-DFT) method with the 6-311++G(d,p) basis sets. Also, dipole moments and HOMO–LUMO analysis of these molecules are reported here, and the theoretical calculations are correlated with experimental data.

2. Experimental

2.1. Apparatus

Melting points were obtained with an Electrothermal Stuart scientific SPM3 apparatus. IR spectra (KBr) were recorded on a FTIR-Perkin Elmer (Spectrum One) spectrophotometer. ^{1}H and ^{13}C spectra were acquired in $CDCl_3$ and DMSO-d_6 solutions with TMS as internal standard, on a Bruker Avance 300 (operating at 300.13 MHz for ^{1}H and at 75.47 MHz for ^{13}C). All spectrophotometric measurements were conducted at room temperature. UV/Vis absorption spectra were recorded on a Varian CARY 50 spectrophotometer. Fluorescence spectra were recorded on a Varian Cary Eclipse spectrofluorometer. The fluorescence quantum yields (Φ) calculated using as standard the disodium fluorescein salt (Φ = 0.9) according to the conventional formula:

$$\Phi_X = (\Phi_S\ A_S\ F_X\ n_X^2) / (A_X\ F_S\ n_S^2)$$

Where, **A** is the absorbance at the excitation wavelength, **F** the Area under the fluorescence curve and **n** the Refractive index of the solvents used. Subscripts "s" and "x" refer to the standard and to the sample of unknown quantum yield, respectively. The excitation source was Xenon flash lamp.

2.2. General procedure for the synthesis of (2*Z*)-2-(arylimino)-2*H*-chromene-3-carboxamides 3-10.

A mixture of 2-imino-2*H*-chromene-3-carboxamide (**1)** (1.88 g, 10 mmol) with the appropriate aniline **2** (10 mmol) and acetic acid (5 mL) were vigorously stirred at ambient temperature for the appropriate time (**3, 4** and **9** 120 min; **5** and **7** 15 min; **6** and **8** 10 min; **10** 1440 min). After reaction completion, controlled by tlc, ice-cold distilled water was added. The obtained solid (2*Z*)-2-(arylimino)-2*H*-chromene-3-carboxamides **3-10** were separated by vacuum filtration and then washed with distilled water and ethyl ether.

2.2.1. (2*Z*)-2-(Phenylimino)-2*H*-chromene-3-carboxamide (3).

Yield 80% (2.11 g), m.p. 234-236°C. IR (cm^{-1}): 3245 ($CH_{aromatic}$), 3113 (CH, C=CH), 1708 (C=O), 1590 (C=C); ^{1}H NMR: δ 9.04 (s, 1H, NH), 9.57 (s, 1H, H-4), 10.38 (s, 1H, NH), 8.84 (d, 1H, H-5, *J* 9.0 Hz), 8.60 (d, 1H, H-8, *J* 9.0 Hz), 8.45 (d, 2H, H-6, H-7, *J*8.1 Hz), 8.38-8.30 (m, 3H, H-3', H-4', H-5'), 8.24-8.19 (m, 2H, H-2',6'); ^{13}C NMR: δ 114.7, 115.4, 118.0, 118.8, 123.92, 123.9, 124.7, 126.3, 128.0, 127.2, 129.9, 149.3, 152.9, 153.6, 162.5; MS (ESI^+): m/z 265 (100%) $(M+H)^+$, 287 (5%) $(M+Na)^+$.

2.2.2.(*Z*)-2-[(3-Carbamoyl-2*H*-chromen-2-yliden)amino]benzoic acid (4).

Yield 85% (2.62 g), m.p. 207-208°C. IR (cm^{-1}): 3393 ($CH_{aromatic}$), 3304 (OH, carboxylic acid), 3159 (CH, C=CH), 1694 (C=O), 1576 (C=C); ^{1}H NMR: δ10.23 (s, 1H, COOH), 9.95 (s, 1H, NH), 9.93 (s, 1H, NH), 8.95 (s, 1H, H-4), 8.91-8.87 (m, 4H, H-5, H-6,H-7, H-8), 8.66-8.55 (m, 2H, H-5', H-6'), 8.37-8.29 (m, 2H, H-3', H-4'); ^{13}C NMR: δ 114.7, 115.8, 118.2, 121.0, 124.2, 124.2, 124.7, 129.4, 129.4, 130.3, 132.7, 140.8, 147.5, 152.4, 153.6, 162.5, 167.2; (ESI^+): m/z 309 (100%) $(M+H)^+$, 331 (8%) $(M+Na)^+$.

2.2.3.(*Z*)-2-(4-Methylphenylimino)-2*H*-chromene-3-carboxamide (5).

Yield 85 % (2.36 g), m.p. 237-238°C. IR (cm^{-1}): 3245 ($CH_{aromatic}$), 3165 (CH, C=CH), 1706 (C=O amide), 1673 (C=O), 1597 (C=C); ^{1}H NMR: δ 10.25 (s, 1H, NH), 8.66 (s, 1H, H-4), 6.18 (s, 1H, NH), 7.61-7.51 (m, 2H, H-5, H-8). 6.32-6.14 (m, 6H, H-6, H-7, H-2',6', H-3',5'), 2.46 (s, 3H, CH_3); ^{13}C NMR: δ 21.1, 115.3, 115.3, 115.4, 118.5, 122.8, 122.9, 124.5, 128.1, 129.5, 134.5, 152.6, 153.4, 164.2; (ESI^+): m/z 279 (100%) $(M+H)^+$, 301 (9%) $(M+Na)^+$.

2.2.4. (*Z*)-2-(4-Methoxyphenylimino)-2*H*-chromene-3-carboxamide (6).

Yield 87% (2.54 g), m.p. 239-240°C. IR (cm^{-1}): 3252 ($CH_{aromatic}$), 3120 (CH, C=CH), 1701 (C=O), 1570 (C=C); ^{1}H NMR: δ 10.96 (s, 1H, NH), 9.13 (s, 1H, H-4), 6.73 (s, 1H, NH), 8.30-8.22 (m, 2H, H-5, H-8), 8.07-7.97 (m, 4H, H-2',6', H-3',5'), 7.69 (d, 2H, H-6, H-7, *J*9.00 Hz), 4.61 (s, 3H, OCH_3); ^{13}C NMR: δ 55.4, 113.9, 115.4, 120.6, 121.4, 124.3, 124.6, 129.4, 132.7, 141.3, 153.6, 153.8, 156.8, 164.1; (ESI^+): m/z 295 (100%) $(M+H)^+$, 317 (3%) $(M+Na)^+$.

2.2.5.(*Z*)-2-(4-Bromophenylimino)-2*H*-chromene-3-carboxamide (7).

Yield 85 % (2.98 g), m.p. 263-264 °C. IR (cm^{-1}): 3260 ($CH_{aromatic}$), 3119 (CH, C=CH), 1698 (C=O), 1595 (C=C); ^{1}H NMR:δ 8.18(s, 1H, NH), 8.51 (s, 1H, H-4), 6.95 (s, 1H, NH), 6.80-6.77 (m, 4H, H-5, H-6, H-7, H-8), 6.32-6.14 (m, 4H, H-2',6', H-3',5'); ^{13}C NMR: δ 114.8, 116.4, 118.2, 121.3, 121.7, 124.3, 124.8, 124.8, 129.4, 131.3, 131.6, 141.1, 152.3, 162.4; (ESI^+): m/z 343 (100%) [$(M+H)^+$, ^{79}Br], 345 (100%) [$(M+H)^+$, ^{81}Br], 365 (9%) [$(M+Na)^+$, ^{79}Br], 367 (9%) [$(M+Na)^+$, ^{81}Br].

2.2.6. (*Z*)-2-(3,4-Dichlorophenyl)imino)-2*H*-chromene-3-carboxamide (8).

Yield 83 % (2.76 g), m.p. 236-237°C. IR (cm^{-1}): 3286 ($CH_{aromatic}$), 3127 (CH, C=CH), 1708 (C=O), 1570 (C=C); ^{1}H NMR: δ 10.10 (s, 1H, NH), 9.60 (s, 1H, H-4), 9.03 (s, 1H, NH), 8.87 (d, 1H, H-5, *J* 9.0 Hz), 8.69-8.61 (m, 3H, H-6, H-8, H-6'), 8.40-8.32 (m, 2H, H-7, H-5'), 8.23 (d, 1H, H-2', *J*8.10 Hz); ^{13}C NMR: δ 114.8, 118.2, 121.2, 122.9, 124.3, 129.4, 129.4, 130.2, 130.6, 130.6, 132.9, 141.5, 149.5, 152.3, 152.3, 162.3; (ESI^+): m/z 333 (100%) [$(M+H)^+$, ^{35}Cl], 335 (60%) [$(M+H)^+$, ^{35}Cl, ^{37}Cl], 337 (15%) [$(M+H)^+$, ^{37}Cl], 355 (12%) [$(M+Na)^+$, ^{35}Cl], 357(7%) [$(M+Na)^+$, ^{35}Cl, ^{37}Cl], 359 (3%) [$(M+Na)^+$, ^{37}Cl].

2.2.7. (*Z*)-2-(2,5-Dichlorophenyl)imino-2*H*-chromene-3-carboxamide (9).

Yield 73 % (2.43 g), m.p. 216-217°C. IR (cm^{-1}): 3300 ($CH_{aromatic}$), 3141 (CH, C=CH), 1708 (C=O), 1570 (C=C); ^{1}H NMR: δ 9.76 (s, 1H, NH), 8.91 (s, 1H, H-4), 6.01 (s, 1H, NH), 7.48-7.38 (m, 2H, H-5, H-8), 7.18-7.15 (m, 2H, H-3', H-4'), 7.05-6.99 (m, 3H, H-6, H-7, H-6'); ^{13}C NMR: δ 116.1, 119.1, 120.8, 123.8, 125.4, 125.4, 125.7, 126.6, 130.1, 130.8, 133.7, 143.9, 152.6, 153.8, 164.1; (ESI^+): m/z 333 (100%) [$(M+H)^+$, ^{35}Cl], 335 (60%) [$(M+H)^+$, ^{35}Cl, ^{37}Cl], 337 (15%) [$(M+H)^+$, ^{37}Cl], 355 (12%) [$(M+Na)^+$, ^{35}Cl], 357 (7%) [$(M+Na)^+$, ^{35}Cl, ^{37}Cl], 359 (3%) [$(M+Na)^+$, ^{37}Cl].

2.2.8. (*Z*)-2-(2,4-Dichlorophenyl)imino-2*H*-chromene-3-carboxamide (10).

Yield 80 % (2.65 g), m.p. 247-248°C. IR (cm^{-1}): 3314 ($CH_{aromatic}$), 3162 (CH, C=CH), 1708 (C=O), 1570 (C=C); ^{1}H NMR: δ 9.16 (s, 1H, NH), 8.62 (s, 1H, H-4), 8.04 (s, 1H, NH), 7.83 (d, 1H, H-6', 8.4 Hz), 7.68 (s, 1H, 3'-H), 7.59-7.21 (m, 4H, H-5, H-6, H-7, H-8), 7.18 (d, 1H, H-5', *J*8.7 Hz); ^{13}C NMR: δ 115.2, 118.5, 121.1, 124.8, 127.3, 127.3, 127.7, 128.5, 128.8, 129.9, 133.4, 140.9, 142.3, 150.2, 152.5, 162.4; (ESI^+): m/z 333 (100%) [$(M+H)^+$, ^{35}Cl], 335 (60%) [$(M+H)^+$, ^{35}Cl, ^{37}Cl], 337 (15%) [$(M+H)^+$, ^{37}Cl], 355 (12%) [$(M+Na)^+$, ^{35}Cl], 357 (7%) [$(M+Na)^+$, ^{35}Cl, ^{37}Cl], 359 (3%) [$(M+Na)^+$, ^{37}Cl].

3. Results and discussion

3.1. UV/vis absorption spectra

The absorption spectra of all the iminocoumarins **3-10** (concentration 10^{-5} M) were recorded immediately after compounds dissolution and filtration through paper. The magnitudes of Stokes shift vary between 4700 and 125900 cm^{-1} and are indicative of a charge transfer transition (Table 1). These spectra in DMSO, DMF, acetonitrile, dichloromethane, THF, ethyl acetate and chloroform displays two distinct bands (Figures 1a-h). The n→π* transition could be located on the carbon 2 carrying the imine function. Indeed the angle C8a-O-C2 is 123.4° [25], which indicates a sp^2 hybridization for the oxygen atom corresponding to free pairs of this atom that occupies a $2p_z$ orbital, thus having a fairly important π character with the core of coumarin. Most certainly, the transition n → π* is completely covered by that of π → π*, which could in part explain the large shoulder obtained around 290 nm. Therefore, the conjugate π electrons system and the electron cloud intensify the stability of the molecules, which explains the low energy of the transitions π→π*.

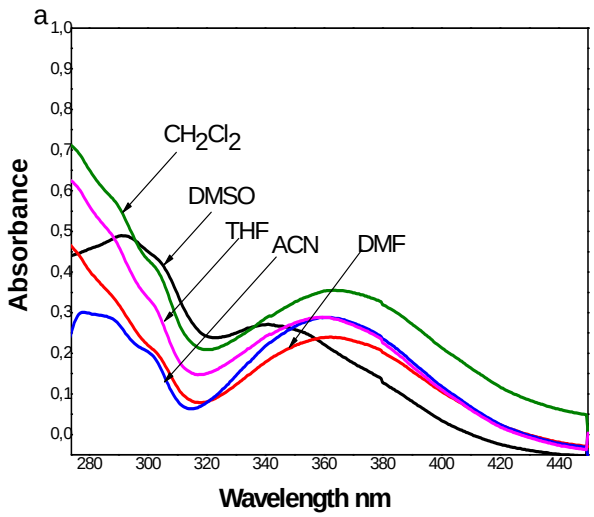

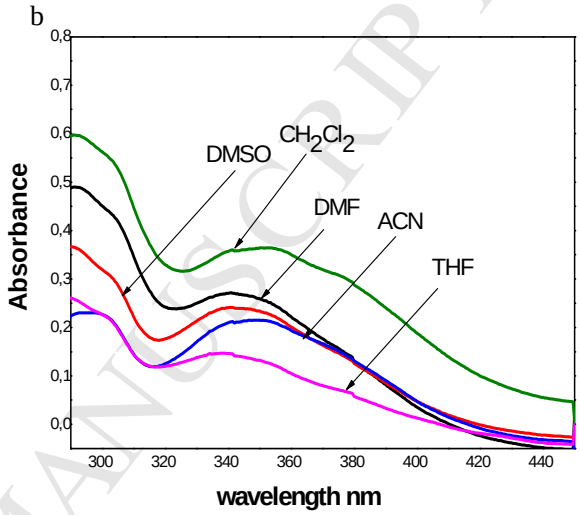

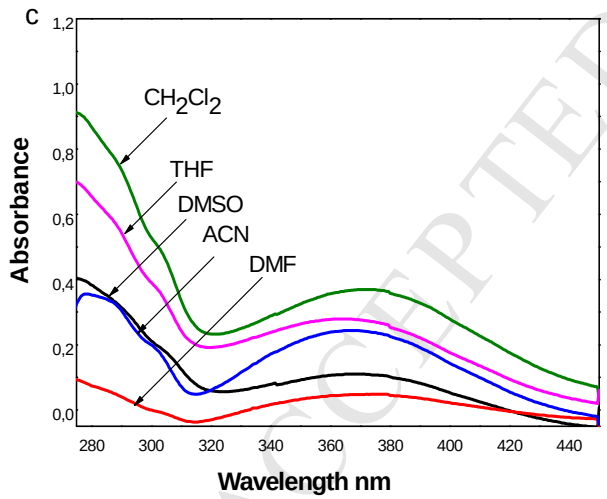

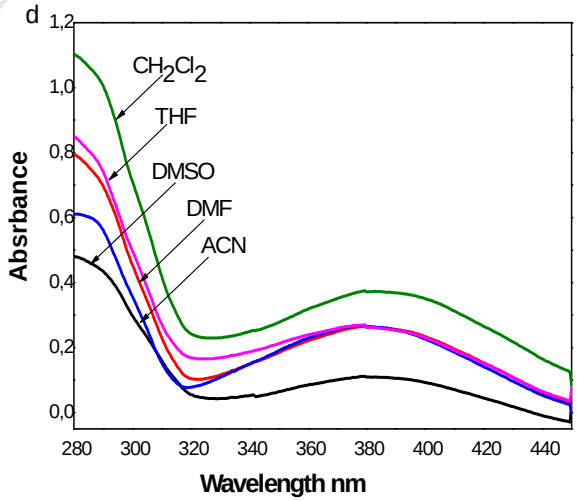

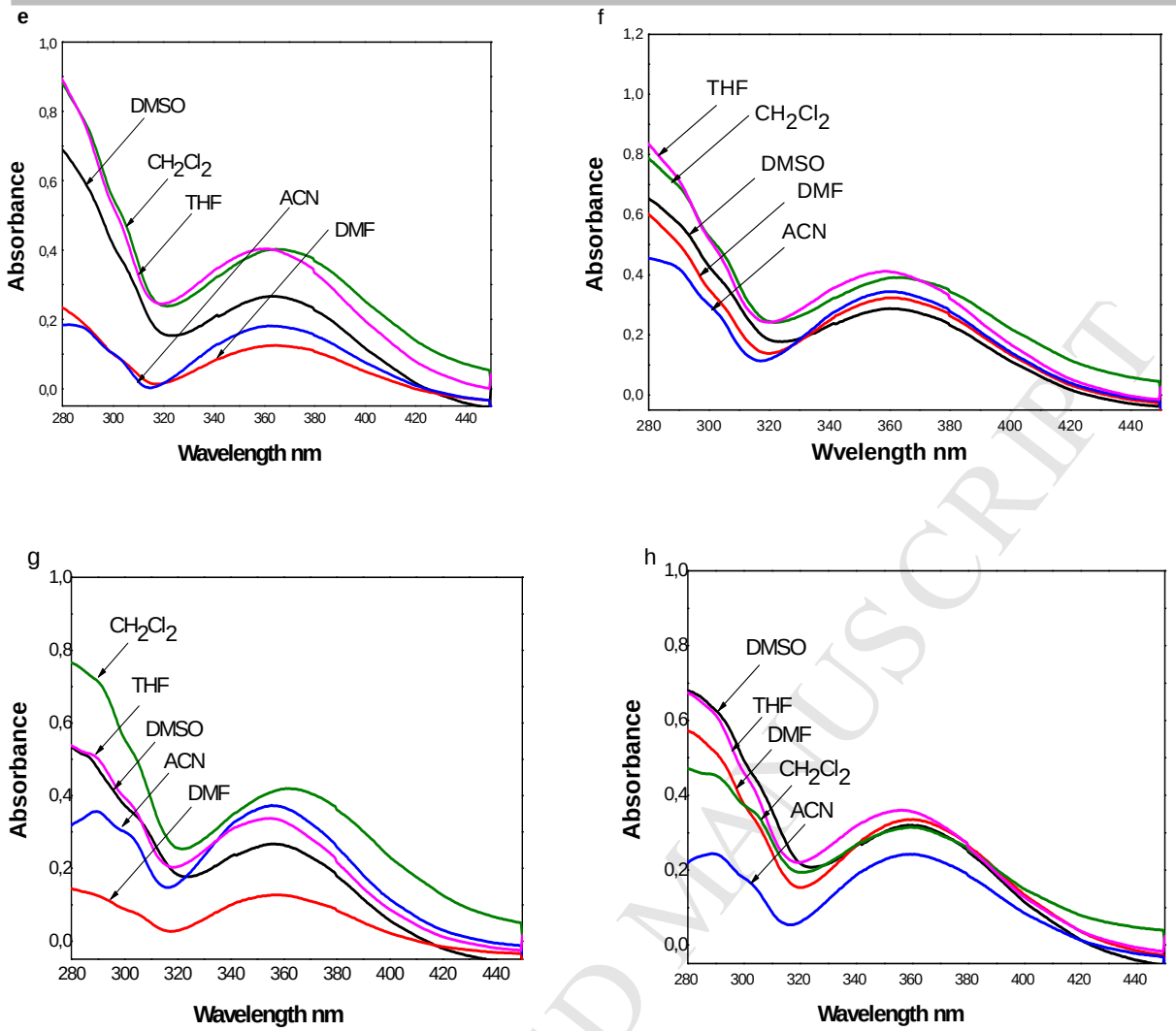

Figures 1a–h: Absorption spectra of all compounds (a) **3**, (b) **4**, (c) **5**, (d) **6**, (e) **7**, (f) **8**, (g) **9** and (h) **10** in different solvents.

3.2. Fluorescence spectra

The fluorescence of iminocoumarins **3-10** in all solvents (10^{-5} M) was acquired at ambient temperature (Table 1).

3.2.1. Steady-state emission spectra

In the emission spectra, the shape and position of all iminocoumarins **3-10** were independent of the excitation wavelength, which confirms that only one specie emits in each solution (Figures 2a-f, Table 1). As example, the spectrum of emission of compound **3** has an emission band at 400 nm in acetonitrile that shifts to 408 nm in chloroform. Compound **4** emits at 347 nm in dichloromethane, at 338 nm in THF and at 334 nm in chloroform.

Table 1 presents the wavelengths of the maxima fluorescence emission bands of their iminocoumarins **3-10** studied at 293K. We note that these iminocoumarins **3-10** do not present an important bathochromic displacement of the fluorescence band, passing from polar solvents to non-polar solvents, since the peaks are almost in the same domain field for all compounds.

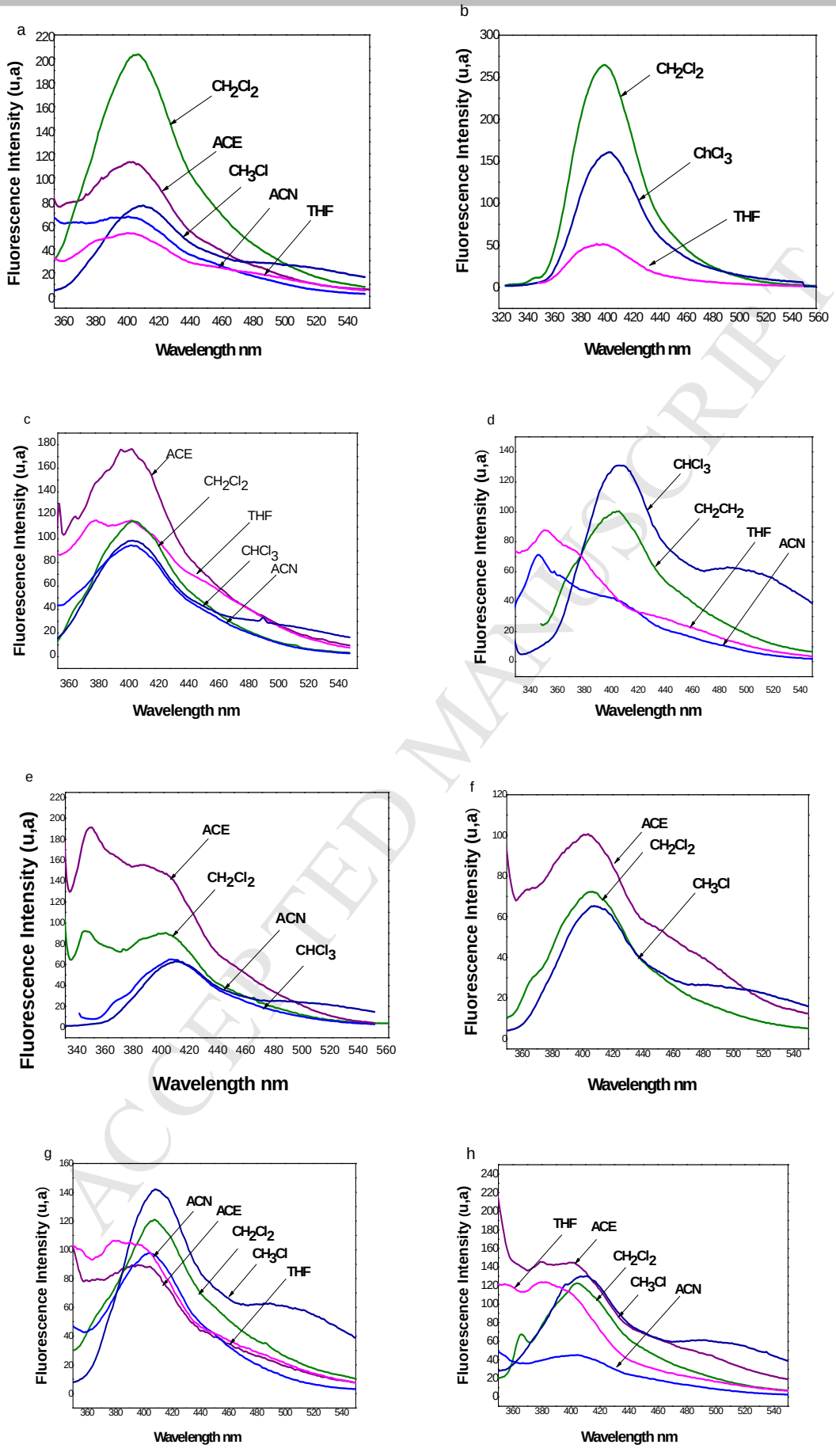

Figures 2.a–h: Emission spectra of all compounds (a) **3**, (b) **4**, (c) **5**, (d) **6**, (e) **7**, (f) **8**, (g) **9** and (h) **10** plotted in different solvents

Table 1: Spectroscopic and photophysical characteristics of the derivatives of compounds **3–10** in different solvents.

Compounds	Solvent	λ_{abs} (nm)	ε (M^{-1} cm^{-1})	λ_{ex} (nm)	λ_{em} (nm)	va-vf (cm^{-1})	Φf
	DMSO	340	26800	310	362	1787.45	0.083
	DMF	361	23600	310	412	3428.99	0.113
	ACN	362	28400	315	400	2624.31	0.048
3	CH_2Cl_2	363	35800	330	407	2978.18	0.086
	THF	364	29000	315	400	2472.53	0.035
	ACE	363	36300	315	402	2672.59	0.062
	$CHCl_3$	333	102000	315	408	5520.23	0.014
	DMSO	342	26800	310	360	1461.99	0.088
	DMF	341	24400	310	404	4573.04	0.162
	ACN	345	21400	315	348	249.87	0.104
4	CH_2Cl_2	347	36200	310	403	4004.55	0.044
	THF	338	15100	310	398	4460.18	0.043
	ACE	342	49700	310	400	4239.77	0.061
	$CHCl_3$	334	49700	310	404	5187.64	0.044
	DMSO	367	11200	315	352	----------	0.087
	DMF	368	4700	310	347	----------	0.549
	ACN	369	24000	315	404	2347.79	0.065
5	CH_2Cl_2	370	36700	330	405	2335.69	0.047
	THF	369	28100	315	404	2347.79	0.086
	ACE	366	52400	315	404	2569.93	0.063
	$CHCl_3$	331	115900	315	405	5520.12	0.016
	DMSO	381	11100	310	351	----------	0.095
	DMF	382	25700	320	405	1486.65	0.053
	ACN	383	26500	315	404	1357.18	0.040
6	CH_2Cl_2	384	37600	330	406	1411.12	0.051
	THF	385	26400	315	400	974.02	0.059
	ACE	380	37100	315	401	1378.13	0.058
	$CHCl_3$	330	111700	315	407	5733.00	0.025
	DMSO	364	26600	310	352	----------	0.084
	DMF	365	12300	315	405	2705.90	0.148
	ACN	366	17900	315	400	2322.40	0.188
7	CH_2Cl_2	367	40900	330	404	2495.48	0.025
	THF	365	39600	315	400	2397.26	0.150
	ACE	360	45500	315	402	2902.15	0.051
	$CHCl_3$	333	125900	315	403	5216.13	0.026
	DMSO	360	28600	310	352	----------	0.044
	DMF	361	32400	320	405	3009.47	0.072
	ACN	362	34100	315	402	2748.69	0.053
8	CH_2Cl_2	363	38700	330	407	2978.18	0.030
	THF	360	40500	315	403	2963.88	0.094
	ACE	360	41800	315	404	3025.30	0.054
	$CHCl_3$	334	111600	315	408	5430.31	0.011
	DMSO	356	26500	310	352	----------	0.055
	DMF	357	12500	320	405	3319.85	0.208
	ACN	358	36700	315	404	3180.48	0.041
9	CH_2Cl_2	362	41800	320	408	3114.50	0.050
	THF	354	33400	315	400	3248.59	0.061
	ACE	353	50700	315	401	3390.96	0.031
	$CHCl_3$	333	121000	315	408	5520.22	0.024
	DMSO	360	32100	310	353	----------	0.062
	DMF	361	33300	320	404	2948.35	0.055
	ACN	358	24000	315	402	3057.34	0.147
10	CH_2Cl_2	360	31200	330	404	3025.30	0.056
	THF	356	35900	315	400	3089.89	0.067
	ACE	355	39700	315	402	3293.39	0.067
	$CHCl_3$	333	118700	315	410	5639.79	0.024

Absorbance wavelength; **ε**: Corresponding molar extinction coefficient; λ_{ex}: Maximum excitation wavelength; λ_{em}: Maximum emission wavelength and shoulders; ν_a-ν_f: Stokes shift; and Φ_f: Fluorescence quantum yield with excitation at the maximum absorption wavelength.

3.3. Theoretical calculations of the ground-state dipole moments

3.3.1. Computational methods:

Calculations have been performed by using Kohn–Sham's DFT and the gradient-corrected hybrid density functional B3LYP [26–28]. This functional is obtained by coupling the three parameters non-local exchange potential of Beck with the non-local correlation functional of Lee *et al.* [29,30]. The complete geometry optimization–is done on a set of this functional and the 6-311++G(d,p) [31,32] basis set as implemented by Gaussian 03W package in gas phase [25]. The solvents were modelled using their dielectric constant employing the CPCM solvation model; calculations were realized as single points on the gas phase geometries. The characterization of electronic transitions and excited states were realized thanks to the time-dependent DFT method (TD-DFT) on their correspondingly optimized ground state geometry. The method, is enough precise to determine the excited states of low molecules and aims to evaluate both the physical and chemical constraints. In order to reproduce the experimental results, vertical excitation energies were calculated for the first 20 singlet excited states.

3.3.2. Geometry

To depict the 3D structure of each compound, we studied the geometry of our compounds using DFT/6-311++G(d,p), under vacuum in different solvents. In order to have the most stable conformation molecular for each compound, we have studied the geometry of various rotamers, when they exist, and calculated their relative energies (Table 2). These relative energies show a little energy difference between rotamers, which indicates the presence of many rotamers in the samples at ambient temperature except for compound **4**. The hydrogen bond, in this case, excludes the existence of both rotamers **4a** and **4b**. Structure **4b** seems the most stable in vacuum in all solvents which is probably due to its shorter O···HN distance 2.153 Å comparing to O····HN distance 2.990 Å in structure **4a**. The use of different solvents significantly change the hierarchy between rotamers' stability of all compounds. The relative energies of rotamers stay very small.

Table S1 (see supporting information) shows the optimized parameters of the most stable rotamers of iminocoumarins **3-10**, under vacuum and figure 3 shows the numbering of the atoms in structure-**3**. The calculated CC, CH, CO and CN bond distances are almost unchanged in all compounds. The influence of the different substituents on all bond lengths seems to be negligible. The hydrogen bond N18…H31 varies between 1.946 Å and 1.975 Å for the compounds **3, 5-10**. This bond appears longer in the case of compound **4** (2.089 Å) since the interaction between H31 and the oxygen of the carboxylic acid group which weakens the hydrogen bond N18…H31 (figure 4; structure-**4b**). The bond angles vary with the electronegativity of the central atom. For example, in all structures, the high electronegativity of oxygen induced the largest value of the C3-O15-C13 bond angle. As for the bond lengths, the substitution of the hydrogen atoms of the phenyl group by the chlorine, bromine, methyl group, metoxy group or carboxylic acid group have not a great influence on the value of the different bond angles.

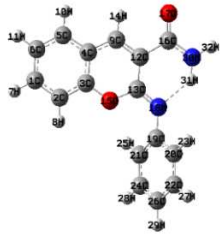

Figure 3: The numbering of the atoms of structure-**3**.

The substituted phenyl moieties in **4-10** structures are more tilted than non-substituted phenyl ring in structure-**3** as is apparent from the values of torsion angle C13-N18-C19-C21 in the different structures. This inclination indicates interactions between the different substituents and oxygen O15. Indeed, the phenyl group of compound **9a** is the most inclined because of the strong repulsions between chlorine bonded to carbon C21 and oxygen O15.

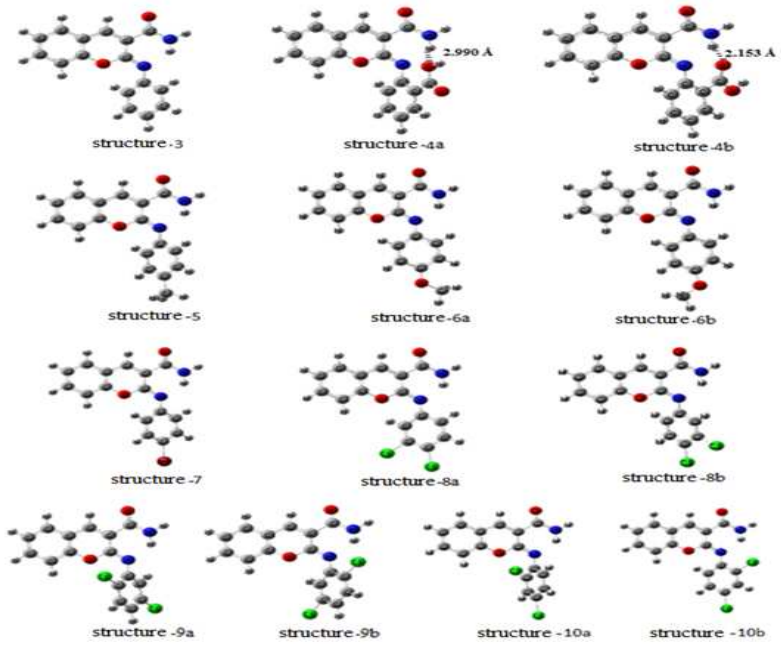

Figure 4. Optimized structures of iminocoumarins **3-10** at the B3LYP/6–311++G(d,p) theory level.

Table 2. Relative energies ΔE (cal/mol) and dipole moment (Debye) of studied molecules calculated at the B3LYP/6–311++G(d,p) theory level.

Compounds	Gas phase (ε 1.0000)		ACN (ε 5.6880)		CH_2Cl_2 (ε 8.9300)		THF (ε 7.4257)		EAC (ε 5.9867)		$CHCl_3$ (ε 4.7113)	
	ΔE	μ	ΔE	μ	ΔE	μ	ΔE	μ	ΔE	μ	ΔE	μ
3	–	3.88	–	5.10	–	4.95	–	4.92	–	4.87	–	4.80
4a	0.46	4.54	0.37	6.06	0.45	5.88	0.44	5.84	0.46	5.77	0.49	5.69
4b	0.00	5.22	0.00	7.08	0.00	6.85	0.00	6.80	0.00	6.72	0.00	6.61
5	–	4.15	–	5.46	–	5.31	–	5.27	–	5.21	–	5.14
6a	0.00	3.78	0.00	4.70	0.00	4.60	0.00	4.57	0.00	4.53	0.00	4.48
6b	0.06	5.21	0.05	6.65	0.06	6.66	0.07	6.61	0.07	6.54	0.08	6.44
7	–	3.48	–	4.56	–	4.44	–	4.41	–	4.36	–	4.30
8a	0.00	3.06	0.00	3.89	0.00	3.80	0.00	3.78	0.00	3.75	0.00	3.70
8b	0.03	4.70	0.01	6.16	0.03	6.00	0.04	5.96	0.04	5.90	0.05	5.81
9a	0.00	3.81	0.00	5.07	0.00	4.92	0.00	4.88	0.00	4.83	0.00	4.76
9b	0.30	3.97	0.31	5.20	0.30	5.06	0.30	5.02	0.30	4.97	0.30	4.90
10a	0.31	3.57	0.34	4.66	0.32	4.54	0.32	4.51	0.31	4.46	030	4.40
10b	0.00	4.60	0.00	6.14	0.00	5.96	0.00	5.92	0.00	5.85	0.00	5.76

3.3.3. Dipole moment

The dipole moment is a significant electronic parameter that results from non-uniform distribution of charges on the different atoms of a given molecules. It is calculated using the B3LYP/6–31++G(d,p) level of theory in gas phase and various solvents are shown in Table 2. As can be note there is an important difference in the dipole moment, while passing from gas to solvent phase environments. Dipole moments have important values in the solvent phase, which may be because of the interactions between the solvent molecules and the dipolar moment of the compounds. The dipole moments increase with dielectric constant in the following order: gas phase < $CHCl_3$< EAC < THF < CH_2Cl_2< ACN.

3.3.4. Frontier Molecular Orbitals

The Highest Occupied Molecular Orbital (HOMO) and Lowest Unoccupied Molecular Orbital (LUMO) are the principal orbitals participating in the chemical stability and chemical reactivity [33-36]. The absorbance and emission of a fluorescent compound are directly related to the energy of these electronic transitions. To provide a reasonable qualitative indication of the excitation properties, HOMO and LUMO for the iminocoumarins **3-10** were investigated. The HOMO and LUMO energies and HOMO–LUMO band gaps were predicted from the B3LYP method to investigate the solvent effects on these energies and band gaps (Table 3). It can be note that the computed energies and the HOMO–LUMO energy gap slightly related to the nature of solvent. The extended conjugated π-systems of iminocoumarins **3-10** decrease the HOMO-LUMO gap resulting in lower energy electron transitions to produce visible light emissions. This low energy gap justifies the eventual charge transfer interaction taking place within these compounds, which is responsible for their light emitting properties.

Table 3: Energies of HOMO, LUMO and gaps $\Delta E_{|HOMO-LUMO|}$ (eV) of the most stable rotamers, calculated at the B3LYP/6–311++G(d,p) theory level.

Compounds	Gas phase	ACN	CH_2Cl_2	THF	EAC	$CHCl_3$
Structure **3**						
HOMO	-6.098	-6.140	-6.135	-6.132	-6.132	-6.129
LUMO	-2.488	-2.466	-2.467	-2.468	-2.468	-2.469
Gap	3.610	3.674	3.668	3.664	3.664	3.660
Structure **4b**						
HOMO	-6.247	-6.277	-6.273	-6.273	-6.272	-6.270
LUMO	-2.469	-2.490	-2.486	-2.485	-2.483	-2.482
Gap	3.778	3.787	3.787	3.788	3.789	3.788
Structure **5**						
HOMO	-5.931	-5.988	-5.891	-5.980	-5.977	-5.974
LUMO	-2.443	-2.447	-2.445	-2.444	-2.444	-2.443
Gap	3.488	3.541	3.446	3.536	3.533	3.531
Structure **6a**						
HOMO	-5.658	-5.740	-5.730	-5.728	-5.725	-5.720
LUMO	-2.394	-2.427	-2.422	-2.421	-2.420	-2.417
Gap	3.264	3.313	3.308	3.307	3.305	3.303
Structure **7**						
HOMO	-6.162	-6.973	-6.154	-6.155	-6.155	-6.156
LUMO	-2.618	-2.506	-2.517	-2.519	-2.523	-2.529
Gap	3.544	4.467	3.637	3.636	3.632	3.627
Structure **8a**						
HOMO	-6.310	-6.269	-6.258	-6.260	-6.262	-6.266
LUMO	-2.705	-2.543	-2.566	-2.570	-2.575	-2.583

Gap	3.605	3.726	3.692	3.690	3.687	3.683
Structure **9a**						
HOMO	-6.579	-6.330	-6.336	-6.337	-6.339	-6.342
LUMO	-2.636	-2.570	-2.581	-2.584	-2.588	-2.593
Gap	3.943	3.760	3.755	3.753	3.751	3.749
Structure **10b**						
HOMO	-6.305	-6.257	-6.262	-6.264	-6.266	-6.268
LUMO	-2.684	-2.551	-2.564	-2.567	-2.572	-2.578
Gap	3.621	3.706	3.698	3.697	3.694	3.690

3.4. Evaluation of the dipole moments

The effect of the electric field (internal or external) on its spectral bands position for the molecule in the excited state is used to determine its dipole moment. The maxima of the absorption and fluorescence bands are used to evaluate the excitation state dipole moments of solutions of compounds **3-10** in the selected solvents. To have a better evaluation of the dipole moments of the excited molecules, we used the equations [Eqs. (1) and (2)] given by Kawski and Bojarski [23-37-38]:

The difference $\bar{\nu}_a - \bar{\nu}_f$:

$$\bar{\nu}_a - \bar{\nu}_f = S_1 f(\varepsilon, n) + const \qquad \text{Eq. (1)}$$

and the sum $\bar{\nu}_a + \bar{\nu}_f$:

$$\bar{\nu}_a + \bar{\nu}_f = -S_2 \Phi(\varepsilon, n) + const \qquad \text{Eq. (2)}$$

Where:

$$\Phi(\varepsilon, n) = f(\varepsilon, n) + 2g(n) \qquad \text{Eq. (3)}$$

and $$g(n) = \frac{3}{2}\frac{n^4 - 1}{(n^2+2)^2} \qquad \text{Eq. (4)}$$

$\bar{\nu}_a$ and $\bar{\nu}_f$ are the absorption and fluorescence maxima (cm^{-1}), respectively. In equation (5) and (6) ε and n represent the dielectric constant and the refractive index of the solvent, respectively. The values of the solvent parameters $f(\varepsilon, n)$ and $\Phi(\varepsilon, n)$ are given by Kawski et al. [21]:

$$f(\varepsilon, n) = \frac{2n^2+1}{n^2+2}\left[\frac{\varepsilon - 1}{\varepsilon + 2} - \frac{n^2-1}{n^2+2}\right] \qquad \text{Eq. (5)}$$

$$\Phi(\varepsilon, n) = \left(\frac{2n^2+1}{(n^2+2)}\left(\frac{\varepsilon-1}{\varepsilon+2} - \frac{n^2-1}{n^2+2}\right) + \frac{3(n^4-1)}{(n^2+2)^2}\right) \qquad \text{Eq. (6)}$$

The values of solvent polarity parameters $f(\varepsilon, n)$ and $\Phi(\varepsilon, n)$ are given in the table 4.

Table 4: Summary of solvent properties and calculated values of solvent polarity parameters $f(\varepsilon, n)$ and $\Phi(\varepsilon, n)$.

Solvent	μ	ε	n	$f(\varepsilon, n)$	$\Phi(\varepsilon,$
ACN	3.45	37.5	1.344	0.863	1.331
CH_2Cl_2	1.14	8.9	1.421	0.596	0.581
THF	1.75	7.58	1.407	0.549	1.102
EAC	1.88	6.02	1.372	0.489	0.996
$CHCl_3$	1.15	4.81	1.446	0.371	0.972

The slopes S1 and S2 are given from Eqs (1) and (2):

$$S_1 = \frac{2(\mu_e - \mu_g)^2}{hca_0^3} \qquad \text{Eq. (7)}$$

$$S_2 = \frac{2(\mu_e^2 - \mu_g^2)}{hca_0^3} \qquad \text{Eq. (8)}$$

Where μ_g and μ_e are ground- and excited-state dipole moments of the solute molecule. h and c are respectively the Planck constant and the light velocity.

a_0 is the Onsager cavity radius of the solute compound and its values was obtained from the equation of Suppan [39,40]: $a_0 = (3M/4\pi\delta N)^{1/3}$, where δ is the density of the solute molecule, M and N the molecular weight of solute and the Avogadro's number, respectively. The ground- and excited-state dipole moments are estimated from Eqs. 9-11. Based on Eqs. (7) and (8) and assuming that the symmetry of the iminocoumarins **3-10** remains unchanged upon electronic transition and the ground- and excited-state dipole moments are parallel, one obtains:

$$\mu_g = \frac{|S_2 - S_1|}{2}\left(\frac{hca_0^3}{2S_1}\right)^{1/2} \qquad \text{Eq. (9)}$$

$$\mu_e = \frac{|S_2 + S_1|}{2}\left(\frac{hca_0^3}{2S_1}\right)^{1/2} \qquad \text{Eq. (10)}$$

$$\frac{\mu_e}{\mu_g} = \frac{|S_2 + S_1|}{|S_2 - S_1|} \quad \text{Slope S2 > Slope S1} \qquad \text{Eq. (11)}$$

The slopes S_1 and S_2 were determined by tracing $(\bar{\nu}_a - \bar{\nu}_f)$ and $(\bar{\nu}_a + \bar{\nu}_f)$ according to $f(\varepsilon, n)$ and $\Phi(\varepsilon, n)$ respectively, for different solvents.

The absorption and emission maxima, Stokes shift $(\bar{\nu}_a - \bar{\nu}_f)$ and arithmetic mean of Stokes shift $(\bar{\nu}_a + \bar{\nu}_f)$ for all the molecules in different solvents are depicted in Table S2 (see supporting information). Typical absorption and emission spectra of the molecules are reported in Table 1.

The correlation coefficients slopes and intercepts of the fitted lines calculated from figures S1.a–h and S2.a–h (see supporting information) that present the graph of $(\bar{\nu}_a - \bar{\nu}_f)$ vs $f(\varepsilon, n)$ and $(\bar{\nu}_a + \bar{\nu}_f)$ vs $\Phi(\varepsilon, n)$] are illustrated in Table 5. Good correlation coefficient is obtained for all cases using the Eqs. (9)–(10) and the values are presented in Table 6. The higher values of μ_e and μ_g and the deviation in the dipole moment for the imimocoumarins **3-10** can be understood in terms of their possible resonance structures as show in figure 5; the carboxamide substituent does not produce a considerable change in the π electron mobility of imimocoumarins **3-10**. Upon excitation, the imine group becomes strong electron donors, which explain the greatest value of dipole moment in

the excited state during the discrepancies between the experimental and theoretical excited dipole moment result from the Kawski and all equation's [20] used for treatment of solvatochromic effect (Table 6) and at B3LYP/6-31+G(d,p) level of theory in different mediums (Table 2) and explain that the dipole moment of the imimocoumarins molecules depends on the transfer process within the molecule. The imonocoumarins **3-10** fluorophores shows that they are more polarin the excited state than the ground state.

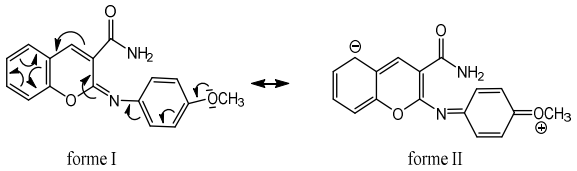

Figure 5. Resonance structure of iminocoumarin **6.**

Table 5: Statistical treatment of the correlations of solvent spectral shifts of iminocoumarins**3-10**.charge transfer.

Compound	Slope	Intercept (cm^{-1})	Correlation coefficient	Number of Data
Eq. (1) correlation				
3	1823.45	1520.89	0.92	5
4	10201.2		0.96	5
	1	9479.81		
5	837.28	1972.51	0.83	5
6	628.75	847.76	0.93	5
7	634.34	2406.15	0.80	5
8	967.68	3551.87	0.95	5
9	2397.75	4522.78	0.87	5
10	1123.11	3927.15	0.80	5
Eq. (2) correlation				
3	120.54	52199.91	0.95	5
4	4914.42	50102.73	0.84	5
5	304.35	50670.59	0.93	5
6	513.11	50473.45	0.82	5
7	397.92	52967.61	0.86	5
8	585.34	51822.30	0.81	5
9	685.90	52292.30	0.80	5
10	361.01	52601.49	0.98	5

Table 6: Ground state, excited state and the variation in the dipole moment.

Compounds	Radius (Å)	μ_g (D)[a]	μ_e (D)[b]	$\Delta\mu$ (D)[c]	μ_e/μ_g[d]
3	4.38	1.82	2.08	0.26	1.14
4	4.45	2.45	6.99	4.54	2.85
5	4.48	0.87	1.86	0.99	2.14
6	4.51	0.22	2.17	1.95	9.86
7	4.45	0.44	1.92	1.48	4.36
8	4.50	0.58	2.37	1.79	4.09
9	4.50	1.66	2.99	1.33	1.80
10	4.50	1.08	2.11	1.03	1.95

[a]The experimental ground-state dipole moment calculated from Eq (9); [b]The experimental excited-state dipole moment calculated from the Eq (10); [c]The dipole moment change calculated from the eq. (7) of Kawski *et al.*; [d]The ratio of μ_e and μ_g is calculated from Eq. (11).
Debye = 3.33564×10^{-30} C m = 10^{-18} esu C m.

4. Conclusion

The solvents effect on the spectrum of UV/Vis and fluorescence emission characteristics of iminocoumarins **3-10** were studied. The results were done in solvent with different polarities indicates a π-π* transition.

The linear correlation of spectral properties with solvatochromic method indicates the role of solute-solvent interactions the dipole-dipole interactions. The first excited state is higher than in the ground state indicating a substantial redistribution of π-electron densities in a more polar excited state of our iminocoumarins **3-10**. This fact indicates the existence of a more relaxed excited state, due to intramolecular charge (ICT). Theoretical ground-state dipole moments of the studied iminocoumarins were predicted using the B3LYP/6–311+G(d,p) level of theory. The results given follow the trend observed in the experimental data. Thus, the determination of the solvatochromic behaviour of the iminocoumarins may provide a valuable tool for the interpretation of their spectroscopic properties. In conclusion, our results assisted with the interpretation of spectroscopic data, refine explicitly the discussions and provide a better understanding of the complex photophysical and photochemical behaviours of the studied iminocoumarins.

Acknowledgments

Thanks are due to University of Aveiro and FCT/MEC for the financial support to the QOPNA research project (FCT UID/QUI/00062/2013), financed by national funds and appropriate co-financed by FEDER under the PT2020 Partnership Agreement, and to the Portuguese NMR Network.

References and notes

[1] D. Egan, R. O'Kennedy, E. Moran, D. Cox, E. Prosser, R. D. Thornes, Drug Metab. Rev. 22 (1990) 503–529.
[2] K. N. Venugopala, V. Rashmi, B. Odhav, Biomed Res. Int. 2013 (2013) 2-14.
[3] T. Kawate, N. Iwase, M. Shimizu, A. S. Stanley, S. Wellington, E. Kazyanskaya, D. T. Hung, Bioorg. Med. Chem. Lett. 23 (2013) 6052–605.
[4] A. Upadhyay, V. K. Singh, R. Dubey, N. Kumar, L. K. Sharma, R. K. P. Singh, Tetrahedron Lett. 58 (2017) 4323–4327.
[5] A. Asres, C. Seyoum, F. Veeresham, S. Bucar, W. Gibbons, D. Wilson, D. Boykin, Phytother. Res.19 (2005) 557-581.
[6] G. Zhang, S. Liu, W. Tan, R. Verma, Y. Chen, D. Sun, Y. Huan, Q. Jiang, X. Wang, N. Wang, Y. Xu, C. Wong, Z. Shen, R. Deng, J. Liu, Y. Zhang , W. Fang, Eur. J. Med. Chem. 129 (2017) 303-309.
[7] R. Frédérik, S. Robert, C. Charlier, J. Ruyck, J. Wouters, B. Pirotte, B. Masereel, L. Pochet, J. Med. Chem. 48 (2005) 7592-7603.
[8] C. Conti, L. P. Monaco, N. Desideri, Bioorg. Med. Chem. 25 (2017) 2074-2083.
[9] X. R. Song, R. Li, H. Ding, R. Yang, Q. Xiao, Y. M. Liang, Tetrahedron Lett. 57 (2016) 4519–4524.
[10] A. N. Vereshchagin, M. N. Elinson, F. V. Ryzhkov, R. F. Nasybullin, S. I. Bobrovsky, A. S. Goloveshkin, M. P. Egorov, Chimie 18 (2015) 1344–1349.
[11] M. Ghate, R. A. Kusanur, M. V. Kulkarni, Eur. J. Med. Chem. 40 (2005) 882-887.
[12] T. Masuda, N. Kawai, Y. Muroya, N. Nakatani, T. J. Mabry, Nat. Prod. Lett. 4 (1993) 129-132.
[13] M. Suzuki, K. Nakagawa-Goto, S. Nakamura, H. Tokuda, S. L. Morris-Natschke, M. Kozuka, Pharm. Biol. 44 (2006) 178–182.
[14] M. A. I. Elbastawesy, B. G. M. Youssif, M. H. Abdelrahman, A. M. Hayallah, Der Pharma Chem. 10 (2015) 337-349.

[15] Z. Guo-Ying, W. Chun-Juan, J. Hanc, L. Yu-Qing, W. Gen-Chun, Phytomedicine 23 (2016) 1814–1820.
[16] Y. Kashman, K. R. Gustafson, R. W. Fuller, J. H. Cardellina, J. B. McMahon, M. J. Currens, R. W. Buckheit, J. Hughes, S. H. Cragg, G. M. Cragg, M. R Boyd, J. Med. Chem. 24 (1992) 2735-2743.
[17] M. Costa, T. A. Dias, A. Brito, F. Proença, Eur. J. Med. Chem. 123 (2016) 487-507.
[18] B. C. Raju, K. Ashok, J. Tiwari, A. Kumar, A. Zehra, B. Sachin, G. A. Saidachary, K. Madhusudana, Bioorg. Med. Chem. 18 (2010) 358-365.
[19] H. Turki, S. Abid, S. Fery-Forgues, R. El Gharbi, Dyes & Pigments 73 (2007) 311-316.
[20] M. Fakhfakh, H. Turki, S. Abid, R. El Gharbi, S. Fery-Forgues, J. Photochem. Photobiol. A: Chem. 185 (2007) 13–18.
[21] Q. Sun, J. Qian, H. Tian, L. Duan, W. Zhang, Chem. Commun. 50 (2014) 8518–8521.
[22] S. K. Chattopadhyay, I. Kundua, R. Maitra, Org. Biomol. Chem. 8 (2014) 8087–8093.
[23] A. Kawski, Solvent-shift effect of electronic spectra and excitation state dipole moments. In: J. R. Rabek (ed.) Progress in photochemistry and photophysics. CRC, New York, 1992, pp 1-47.
[24] A. Benazzouz, M. Makhloufi-Chebli, S. M. Hamdi, B. Boutemeur-Kheddis, Artur M. S. Silva, M. Hamdi, J. Mol. Liq. 219 (2016) 173–179.
[25] M. J. Frisch, G. W. Trucks, H. B. Schlegel, G. E. Scuseria, M. A. Robb, J. R. Cheeseman, J. A. Montgomery, T. Vreven, K. N. Kudin, J. C. Burant, J. M. Millam, S. S. Iyengar, J. Tomasi, V. Barone, B. Mennucci, M. Cossi, G. Scalmani, N. Rega, G. A. Petersson, H. Nakatsuji, M. Hada, M. Ehara, K. Toyota, R. Fukuda, J. Hasegawa, M. Ishida, T. Nakajima, Y. Honda, O. Kitao, H. Nakai, M. Klene, X. Li, J. E. Knox, H. P. Hratchian, J. B. Cross, C. Adamo, J. Jaramillo, R. Gomperts, R. E. Stratmann, O. Yazyev, A. J. Austin, R. Cammi, C. Pomelli, J. W. Ochterski, P. Y. Ayala, K. Morokuma, G. A. Voth, P. Salvador, J. J. Dannenberg, V. G. Zakrzewski, S. Dapprich, A. D. Daniels, M. C. Strain, O. Farkas, D. K. Malick, A. D. Rabuck, K. Raghavachari, J. B. Foresman, J. V. Ortiz, Q. Cui, A. G. Baboul, S. Clifford, J. Cioslowski, B. B. Stefanov, G. Liu, A. Liashenko, P. Piskorz, I. Komaromi, R. L. Martin, D. J. Fox, T. Keith, M. A. Al-Laham, C. Y. Peng, A. Nanayakkara, M. Challacombe, P. M. W. Gill, B. Johnson, W. Chen, M. W. Wong, C. Gonzalez, J. A. Pople, Gaussian 03, Revision A.1, Gaussian Inc, Pittsburgh PA, 2003.
[26] A. D. Becke, Phys. Rev. A 38 (1988) 3098-3100.
[27] A. D. Becke, J. Chem. Phys. 98 (1993) 5648-5652.
[28] A. D. Becke, J. Chem. Phys. 98 (1993) 1372-1377.
[29] C. Lee, W. Yang, R. G. Parr, Phys. Rev. B. Condens. Matter 37 (1988) 785-789.
[30] B. Miehlich, A. Savin, H. Stolt, H. Preuss, Chem. Phys. Lett. 157 (1989) 200-206.
[31] G. A. Petersson, M. A. Al-Laham, J. Chem. Phys. 94 (1991) 6081-6090.
[32] G. A. Petersson, A. Bennett, T. G. Tensfeldt, M. A. Al-Laham, W. A. Shirley, J. Mantzaris, J. Chem. Phys. 89 (1988) 2193-2218.
[33] C. T. Zeyrek, H. Unver, Ö. T. Arpacı, K. Polat, N. O. İskeleli, M. Yildiz, J. Mol. Struct. 1081 (2015) 22-37.
[34] M. Govindarajan, S. Periandy, K. Carthigayen, Spectrochim. Acta A 97 (2012) 411-422.
[35] C. Ravikumar, I. H. Joe, V. S. Jayakumar, Chem. Phys. Lett. 460 (2008) 460-552.
[36] S. Zaater, A. Bouchoucha, S. Djebbar, M. Brahimi, J. Mol. Struc. 1123 (2016) 344-354.
[37] L. Billot, A. Kawski, Zeitsch. Naturfors. 17a (1962) 621-626.
[38] A. Kawski, P. Bojarski, Spectrochim. Acta Part A: Mol. Biomol. Spect. 82 (2011) 527-528.
[39] J. R. Mannekutla, B. G. Mulimani, S. R. Inamdar. Spectrochim. Acta Part A: Mol. Biomol. Spect. 69 (2008) 419–426.
[40] P. Suppan, Chem. Phys. Lett. 94 (1983) 272–275.

Highlights

- A bathochromic shift occurs in the UV-Vis and fluorescence spectra of iminocoumarins with the increase of solvent polarity
- Dipole moments of the excited state are higher than those of the ground state
- A substantial redistribution of the π-electron densities in a more polar excited state is observed
- The small transition energy gap explains the charge transfer interaction within the molecules and their light emitting properties